Supporting information

Tuning ORR Activity via Controllable Dealloying: A Model Study of Ordered Cu_3Pt/C Intermetallic Nanocatalysts

Deli Wang, Yingchao Yu, Huolin L. Xin, Robert M. Hovden, Peter Ercius, Julia A. Mundy, Hao Chen,

Jonah H. Richard, David A. Muller, Francis J. DiSalvo, and Héctor D. Abruña

Materials and Methods

1. Experimental Section

Synthesis of Cu_3Pt/C ordered intermetallic nanoparticles and two dealloying methods

Carbon supported Cu_3Pt ordered intermetallic nanoparticles with 10wt% of Pt were prepared using an impregnation method. In a typical synthesis, 53.3 mg of $H_2PtCl_6 \cdot 6H_2O$ and 41.4 mg of $CuCl_2$ were dissolved in deionized water, and 160.4 mg of Vulcan XC-72 carbon support were dispersed in it. After ultrasonic blending for 30 min, the suspension was heated under magnetic stirring to allow the solvent to evaporate and to form a smooth, thick slurry. The slurry was dried in an oven at 60 ^{o}C. After being ground in an agate mortar, the resulting dark and free-flowing powder was heated in a tube furnace at 300 ^{o}C under flowing H_2/N_2 for 5 h. Finally, the powder was cooled to room temperature under N_2. The as-prepared Cu_3Pt/C powder was then annealed at 1000 ^{o}C under an H_2 atmosphere for 10 h to form an ordered intermetallic phase.

The carbon supported Cu_3Pt ordered intermetallic nanoparticles were dealloyed using two methods: electrochemical and chemical. Electrochemical dealloying was performed by potential cycling of the catalysts between 0.05 V and 1.0 V in 0.1 M $HClO_4$ at a scan rate of 50 mVs^{-1} (for detailed information see the electrochemical testing section). Chemical leaching was conducted by immersing the catalysts in 1 M HNO3 under magnetic stirring at 40 ^{o}C for two days. The sample was then centrifuged and washed using deionized water until the pH value was close to 7.

2. Characterization

The catalysts were characterized by powder X-ray diffraction using a Rigaku® Ultima VI diffractometer, and diffraction patterns were collected at a scanning rate of 5 ^{o}/min and with a step of 0.02 ^{o}. The diffraction peak at around 25° is attributed to the carbon support in the as-prepared Cu_3Pt/C.

The TEM images and EELS maps were acquired on a 5th-order aberration-corrected scanning transmission electron microscope (Nion UltraSTEM) operated at 100 kV, with a convergence angle α_{max} = ~30 mrad. The upper limit of beam dose was calculated to be 2.0×10^4 e$^-$/(nm^2·s) for each second of electron beam exposure.

3. Electrochemical testing

Electrochemical experiments were carried out in 0.1 M $HClO_4$ at room temperature using a Solartron electrochemistry station. Working electrodes were prepared by mixing the catalyst with Nafion (0.05 wt % Nafion dissolved in ethanol) solution. The mixture was sonicated and about 5.0 µL were applied onto a glassy carbon disk. After solvent evaporation, a thin layer of the Nafion-catalyst-Vulcan ink remained on the GC surface to serve as the working electrode. The Pt loading on the RDE was calculated as 17.7 µg$_{Pt}$ cm^{-2}. A Pt wire was used as the counter electrode and a reversible hydrogen electrode (RHE), in the same electrolyte as the electrochemical cell, was used as the reference electrode. All potentials are referred to the RHE. For the electrochemical surface area (ECSA) study, cyclic voltammetry (CV) was conducted within the potential range of +0.05 V to +1.00 V at a scan rate of 50 mVs^{-1} in 0.1 M $HClO_4$. ECSA values were calculated by integrating the area under curve for the hydrogen adsorption region between +0.05 and +0.40 V for the reverse sweep in the CV and using a conversion factor of 0.21 mCcm^2. The oxygen reduction reaction (ORR) polarization curves were obtained by sweeping the potential from +0.20 to +1.10 V at a scan rate of 5 mV s^{-1} and at a rotation rate of 1600 rpm. The Koutecky-Levich equation was used to calculate kinetic current densities based on the ORR polarization curves, and which can be described as:

$$\frac{1}{I} = \frac{1}{I_d} + \frac{1}{I_k}$$

Where I is the overall current density, which is the experimentally measured current; I_d is the diffusion-limited current density and I_k is the kinetic current density.
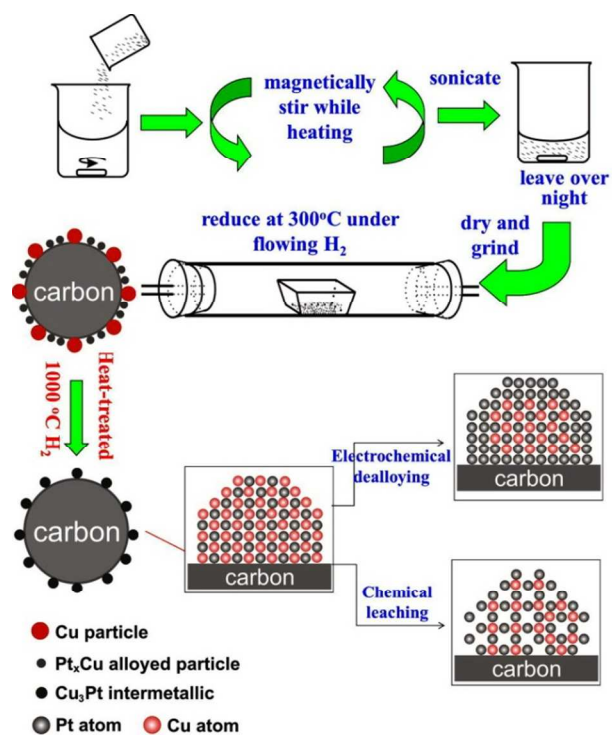
Figure S1. Schematic depiction of the synthesis procedure of Cu_3Pt/C ordered intermetallic nanoparticles and the two dealloying methods employed.
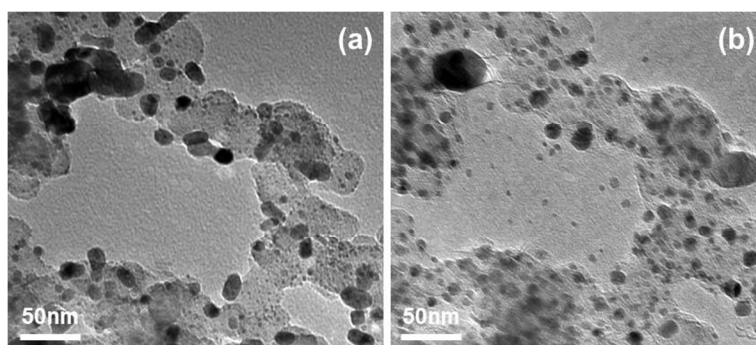

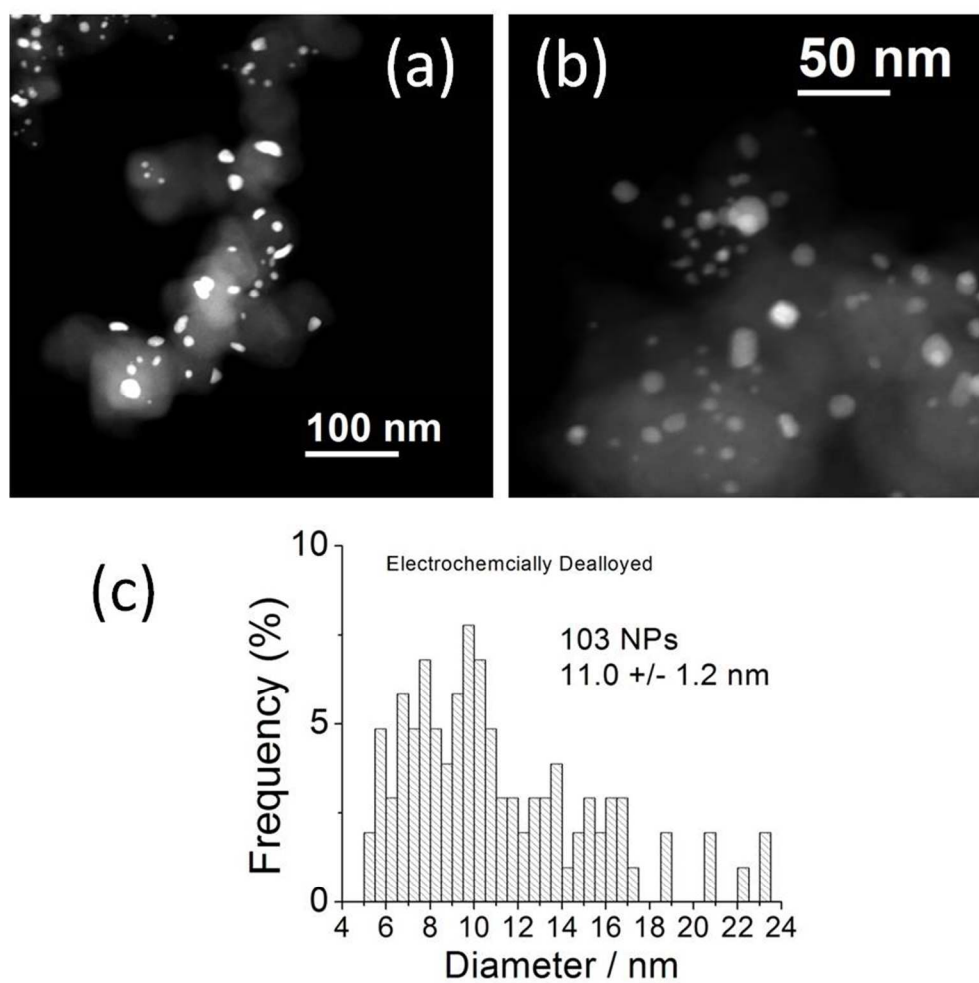Figure S2. TEM images of *in-situ* heating experiment before(a) and after(b) 1000^oC heat-treated.

Figure S3. ADF-STEM images (a and b) of electrochemically dealloying nanoparticles and particle size distribution.
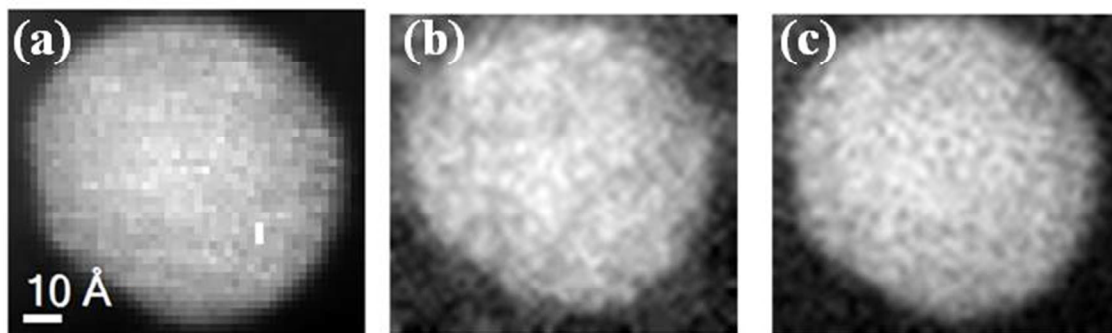
Figure S4. Comparison of the relibility of MCR (multivariate curve resolution) analysis of Pt N_3 edge, for the nanoparticle presented in Figure 4. (a) annular dark field (ADF) image; (b) simultaneously recorded Pt-M edge; (c) 20 iterations of MCR analysis of Pt-N_3 edge. Due to 'Z-contrast', the ADF signal should correspond mostly to Pt (but not Cu). Since the Pt-M edge has delayed and broad onset peaks, the power-law background substraction method results in a very noisy Pt map (figure s6(b)). In contrast, the MCR method can yield ca. 10 times better signal-to-noise ratio. By comparing the ADF signal and Pt-M edge maps with the MCR method, no discrepancies were found, indicating the reliability of such method[1,2].
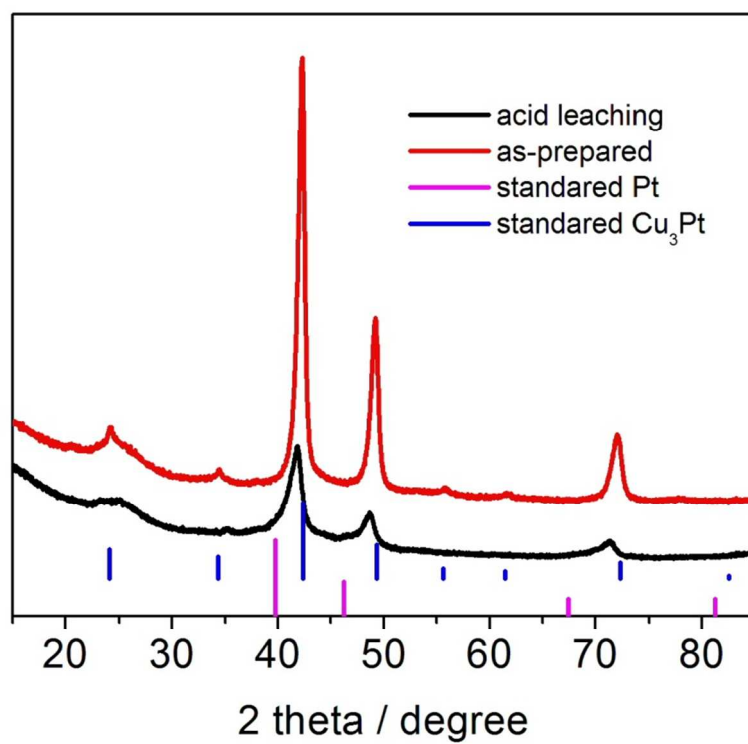
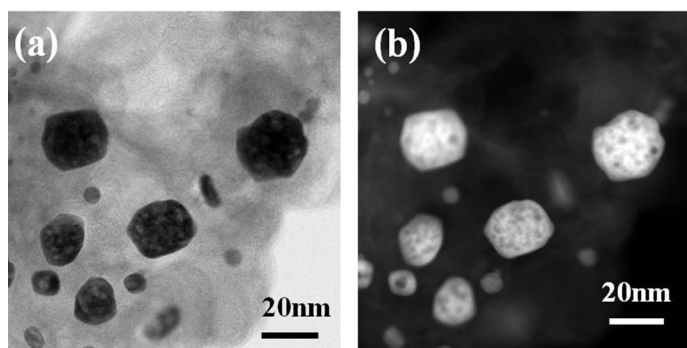Figure S5. XRD patterns of Cu$_3$Pt/C ordered intermetallic nanoparticles before and after chemical leaching.

Figure S6. BF (a) and ADF-STEM (b) images of chemically leached nanoparticles after 5000 potential cycles in 0.1 M HClO4 between 0.05 and 1.0 V at a scan rate of 50 mVs^{-1}.
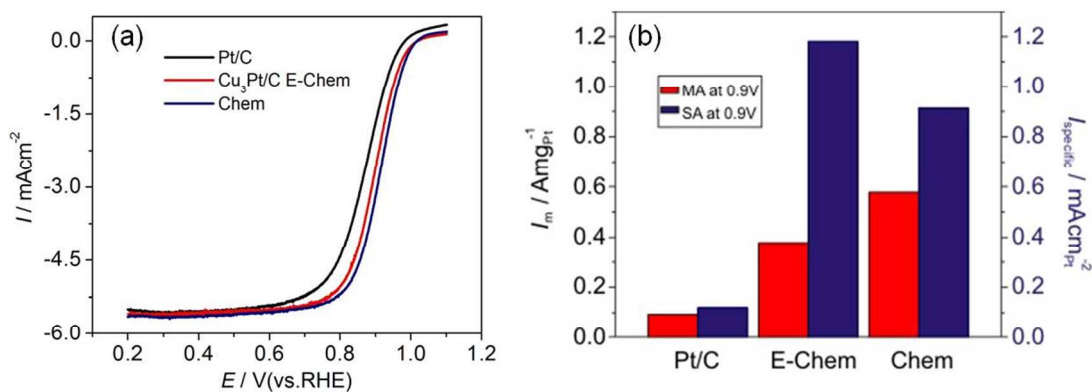
Figure S7. Comparison of the ORR activities between chemically and electrochemically dealloyed nanoparticles. (a) ORR polarization curves in O_2-saturated 0.1 M $HClO_4$, at a rotation rate of 1600 rpm and a scan rate of 5 mVs^{-1}. (b) Mass and specific activities at +0.9 V. (The ORR activities tested after 50 potential cycles between +0.05 to +1.0 V in 0.1 M $HClO_4$.)

References

1. Yu, Y.; Xin, H. L.; Hovden, R.; Wang, D.; Rus, E.; Mundy, J. A.; Muller, D. A.; Abruña, H. D., 3-D Tracking and Visualization of Hundreds of Pt-Co Fuel Cell Nanocatalysts During Electrochemical Aging. *Nano Letters* **2011,** *Article ASAP. DOI:10.1021/nl203920s.*

2. Xin, H. L.; Mundy, J. A.; Liu, Z.; Cabezas, R.; Hovden, R.; Kourkoutis, L. F.; Zhang, J.; Subramanian, N. P.; Makharia, R.; Wagner, F. T.; Muller, D. A., Atomic-Resolution Spectroscopic Imaging of Ensembles of Nanocatalyst Particles Across the Life of a Fuel Cell. *Nano Letters* **2011,** *12* (1), 490-497.